

# Synthesis of SiC nano-powder from organic precursors using RF inductively coupled thermal plasma

Sang-Min Ko<sup>a,b</sup>, Sang-Man Koo<sup>b</sup>, Woo-Seok Cho<sup>a</sup>, Kwang-Take Hwnag<sup>a</sup>, Jin-Ho Kim<sup>a,\*</sup>

<sup>a</sup> *Icheon Branch, Korea Institute of Ceramic Engineering & Technology (KICET), Icheon-si, Gyeonggi-do, Republic of Korea*

<sup>b</sup> *Department of Chemical Engineering, Hanyang University, Seoul 133-791, Republic of Korea*

Received 14 September 2011; received in revised form 11 October 2011; accepted 11 October 2011

Available online 29 October 2011

## Abstract

Silicon carbide (SiC) has recently drawn an enormous amount of industrial interest owing to useful mechanical properties such as its thermal resistance, abrasion resistance and thermal conductivity at high temperatures. RF inductively thermal plasma (PL-35 Induction Plasma, Tekna Co., Canada) has been utilized for synthesis of fine SiC nano-powder from organic precursors (tetraethylorthosilicate, hexamethyldisilazane and vinyltrimethoxy silane). It was found that powders exposed to thermal plasma consist of SiC with free carbon and amorphous silica (SiO<sub>2</sub>), after a thermal treatment and a HF treatment, the impurities are driven off, resulting in fine SiC nano-powder. The synthesized SiC nano-powder lies between 30 and 100 nm, and the characteristics of its microstructure, phase composition and specific surface are determined by X-ray diffraction (XRD), field emission scanning electron microscopy (FE-SEM), and thermogravimetric (TG) and Brunauer–Emmett–Teller (BET) analyses. © 2011 Published by Elsevier Ltd and Techna Group S.r.l.

**Keywords:** A. Organic precursor; RF inductively coupled thermal plasma processing; Silicon carbide (SiC); Nano-powder

## 1. Introduction

Silicon carbide (SiC) is a non-oxide ceramic engineering materials that has garnered a considerable amount of interest over the past 20 years. It has a wide range of industrial applications due to its excellent mechanical properties, high thermal and electrical conductivity, and excellent chemical oxidation resistance. These properties make silicon carbide an attractive candidate material for many applications, such as grinding materials, polishing paste, wear-resistant materials, catalyst supports, filters for molten metals or hot gases, high temperature structural materials, and as reinforcement in composites [1–3].

The conventional synthesis method of SiC is a carbothermal reduction known as the Acheson process. This has been applied at an industrial scale due to the available of inexpensive raw materials. This process requires several hours of the carbothermal reduction of SiO<sub>2</sub> with carbon powder at temperatures around 2200–2400 °C. Due to the high reaction

temperatures and long reaction times associated with the process, the powders produced have a large particle size and consist of mostly  $\alpha$ -phase SiC. Therefore, it is difficult to prepare ultrafine silicon carbide powders using the Acheson process [4].

In order to meet the stringent requirements of some applications, a series of improved methods has been developed to fabricate ultra-fine silicon carbide powders. For example, sol–gel, SHS, advanced Acheson process, laser and microwave applications have been reported in the literature as having been used in the synthesis of fine SiC powders. However, these methods involve multiple steps and have not readily led commercial viability [5–8].

The RF inductively coupled thermal plasma process presents an attractive route for synthesis of powders in the nanometer size range [9–13]. RF thermal plasma has a high temperature (over 10<sup>4</sup> K) and is rapidly cooled (10<sup>5</sup>–10<sup>6</sup> K/s) in the tail flame region. The high temperature region can provide enough energy for the melting and evaporation of the raw materials and the rapidly cooled tail aids a rapid solidification process. The supersaturation of vapor species, which provides the driving force for particle condensation, can be very high in the plasma tail, leading to the production of ultra-fine particles through

\* Corresponding author. Tel.: +82 31 645 1431; fax: +82 31 645 1488.

E-mail address: [jino.kim@kicet.re.kr](mailto:jino.kim@kicet.re.kr) (J.-H. Kim).

homogeneous nucleation. The plasma gas does not come in contact with the electrodes, which can eliminate possible sources of contamination. Furthermore, the operation environment is flexible from an oxidizing to a reducing atmosphere. Therefore, RF thermal plasma is also an effective means of preparing high-purity powders [11–13].

In this work, pure SiC nano-powder was produced by RF inductively thermal plasma from liquid phase organic precursors. The microstructure, phase composition, specific surface area and free carbon content of the synthesized SiC nano-powders were investigated.

## 2. Experimental

Fig. 1 shows a schematic diagram of the RF inductively thermal plasma used here to synthesize the SiC nano-powders. An RF inductively coupled thermal plasma torch (PL-35 Induction plasma, TEKNA Co., Canada) was connected to a reactor, a cyclone, a filter unit and a vacuum pump. Organic precursors were delivered by a peristaltic pump to an atomizer probe placed in the plasma flame and was injected by a water-cooled probe with a dispersion gas at the center of the plasma torch. The atomized precursor was rapidly dissociated in the plasma flame, and the gaseous products were condensed by rapidly cooling the plasma flow in the reactor. The evacuated gas stream containing the product powder was passed through a cyclone and a filter assembly. The plasma torch was operated with Ar central gas and Ar sheath gas at a constant plate power of 18 kW. The precursor feeding rate and reactor pressure were

Table 1  
Operation condition of RF inductively thermal plasma.

Central gas	Ar, 20 slpm
Dispersion gas	Ar, 5 slpm
Sheath gas	Ar, 60 slpm
Quenching gas	N <sub>2</sub> , 150 slpm
Plate power	18 kW
Reactor pressure	15 psi
Feed rate	19.5 ml/min

kept at 19.5 ml/min and 15 psi, respectively. The other experimental conditions, such as the flow rates of the plasma central gas, the sheath gas, the dispersion gas and the quenching gas, were kept constant. The effect of the precursors on the synthesis of the SiC nano-powders was investigated. Typical experimental conditions are listed in Table 1. In the experiments, tetraethylorthosilicate (C<sub>8</sub>H<sub>20</sub>O<sub>4</sub>Si, >98.0%, SAMCHUN), hexamethyldisilazane (C<sub>6</sub>H<sub>19</sub>NSi<sub>2</sub>) and vinyltrimethoxysilane (C<sub>5</sub>H<sub>12</sub>O<sub>3</sub>Si) were used as the precursors.

Free carbon was found with the synthesized SiC nano-powders. The free carbon was driven off by a heat treatment at 800 °C. After the heat treatment, amorphous silica (SiO<sub>2</sub>) was found and was driven off by a HF treatment.

The synthesized SiC nano-powders were characterized in terms of their phase composition, microstructure, specific surface area and particle size. An X-ray diffractometer (XRD, D/MAX2500VL/PC, Rigaku, Japan) was used to analyze the phase composition and crystallite size of particles. The particle morphology and the primary size of particles were observed by

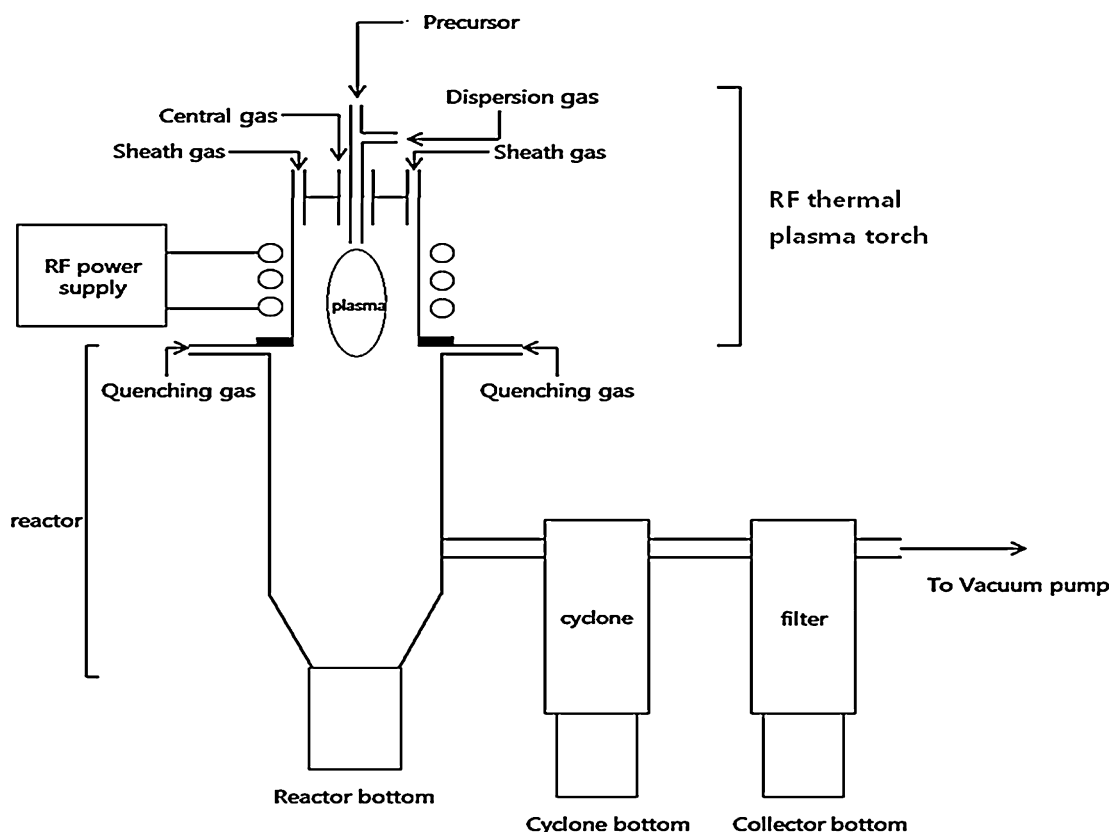


Fig. 1. Schematic diagram of thermal plasma system for preparation of SiC nano-powder.

using a field emission scanning electron microscope (FE-SEM, JSM-7001F, JEOL, Japan). The specific surface area was determined by nitrogen adsorption using BET (BelsorpII mini, BEL, Japan) method. The mean particle size was calculated from measured specific surface area. The temperature after the treatment was determined by a TG analysis (TG, DTG-60H, SHIMADZU).

### 3. Results and discussion

#### 3.1. Microstructure and crystalline phase characterization

XRD patterns of the synthesized powders created using RF inductively thermal plasma are shown in Fig. 2. The XRD patterns of synthesized powders clearly confirm the formation of  $\beta$ -SiC. The major peaks of all synthesized SiC nano-powder at diffraction angles ( $2\theta$ ) of  $35.6^\circ$ ,  $41.3^\circ$ ,  $60.1^\circ$ ,  $72.1^\circ$  are attributed to the (1 1 1), (2 0 0), (2 2 0) and (3 1 1) planes of the cubic  $\beta$ -SiC phase, which indicates that all of the as-synthesized powders are mainly composed of  $\beta$ -SiC nanosized grains. At the same time, the  $\alpha$ -SiC phase and amorphous carbon phase were detected at diffraction angles of  $33.6^\circ$  and approximately  $25^\circ$ , respectively.

The crystalline grain size of the synthesized SiC nano-powders was calculated with the Scherrer formula:

$$d = \frac{0.89\lambda}{\beta \cos \theta} \quad (1)$$

Here  $d$  is the crystalline grain size,  $\lambda$  is the wavelength of the X-rays (0.154 nm),  $\beta$  is the full-width at half peak height of the diffraction peak and  $\theta$  is the Bragg's angle. It is desirable to use peaks at smaller diffraction angles to reduce the effect of lattice strain [14,15]. The smallest diffraction angle is  $17.8^\circ$  ( $2\theta = 35.6^\circ$ ) as shown in Fig. 2. Therefore, the values of  $L$  of the N-1, N-2 and N-3 powders were determined to be approximately 30.2 nm, 25.3 nm and 47.3 nm, respectively, using Eq. (1).

The synthesized SiC nano-powders were analyzed in terms of their particle size, particle morphology and distribution using a field emission scanning electron microscope (FE-SEM). Fig. 3 shows a FE-SEM micrograph of the synthesized SiC nano-powders. The primary particle size and particle configuration according to the FE-SEM observation and the specific surface area as determined by the BET method are summarized in Table 2. The primary particle size of the N-1 powder was finest among all synthesized SiC nano-powders around 30 nm with a high specific surface areas of  $120.9 \text{ m}^2/\text{g}$ . Its morphology can be characterized by its globosity. The primary particle size

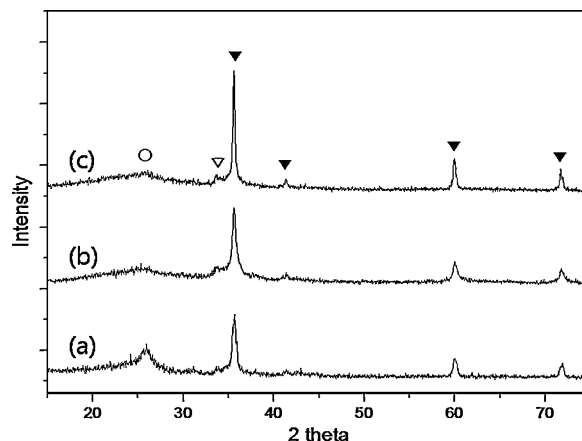


Fig. 2. X-ray diffraction patterns of synthesized SiC nano-powders from (a) N-1, (b) N-2, and (c) N-3.

of the N-2 powder was between 30 and 100 nm with a specific surface areas of  $84.2 \text{ m}^2/\text{g}$  with the same type of morphology. The N-1 and N-2 particles were aggregated. The N-3 powders had two separate categories of particles. The major primary particle size of the N-3 powders was around 30 nm with a globular morphology. A few hexagonal particles around 100 nm in size were also observed. Hexagonal SiC particles included the  $\alpha$ -SiC discussed as part of the XRD analysis (Fig. 2). The specific surface area was  $112.4 \text{ m}^2/\text{g}$ . Assuming the synthesized SiC particles to be spherical, the mean particle size of the synthesized particles can be obtained from the following equation (Table 2):

$$d = \frac{6}{S_{\text{BET}} \rho} \quad (2)$$

Here  $d$  is the mean particle size of the synthesized SiC powders,  $S_{\text{BET}}$  is the specific surface area of the synthesized SiC powders and  $\rho$  is the SiC density (the theoretical density of SiC is  $3.2 \text{ g}/\text{cm}^3$ ). The BET results showed that the mean particle sizes of the N-1, N-2 and N-3 powders are 15.5 nm, 22.3 nm and 16.7 nm, respectively. It was found that the specific surface area and mean particle size was in line with the primary particle size. The mean particle size of the N2 powders was the largest among all of the synthesized SiC nano-powders. Thermal plasma processing involves the evaporation of precursors at the high-temperature region of the plasma, particle nucleation by the supersaturation of vapor species and crystal growth by the high density of the vapor-phase precursors. Therefore, the crystal growth depends on the density of vapor-phase precursors [16]. The density of the vapor-phase precursors of hexamethyldisilazane was higher than that of the other precursors

Table 2

The primary particle size and particle configuration by FE-SEM observation and specific surface area and mean particle size by BET method of synthesized SiC nano-powders.

Designation	Precursor	BET ( $\text{m}^2/\text{g}$ )	Mean particle size (nm)	Primary particle size (nm)	Particle configuration
N-1	Tetraethylorthosilicate	120.9	15.5	20	Spherical
N-2	Hexamethyldisilazane	84.2	22.3	20–100	Spherical
N-3	Vinyltrimethoxysilane	112.4	16.7	20 and 100	Spherical, hexagonal

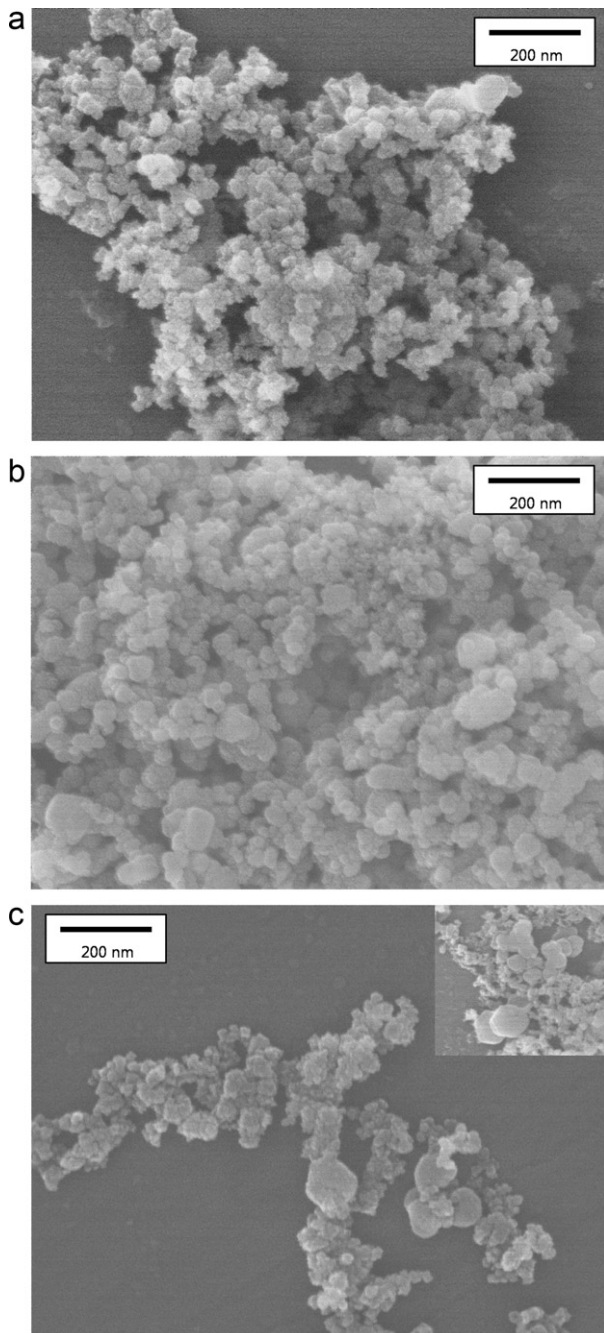


Fig. 3. FE-SEM images of the synthesized SiC particles: (a) N-1, (b) N-2, and (c) N-3.

because the Si in hexamethyldisilazane is twice that of the other precursors. Therefore, the synthesized N2 powders were larger than the other powders.

### 3.2. Effect of a post-treatment process

Free carbon was observed at all of the as-synthesized SiC nano-powders and was driven off via a post-treatment process. The heat treatment temperature was determined in a thermogravimetric analysis. Fig. 4 shows the TG curves of the SiC powder synthesized from tetraethylorthosilicate. The tempera-

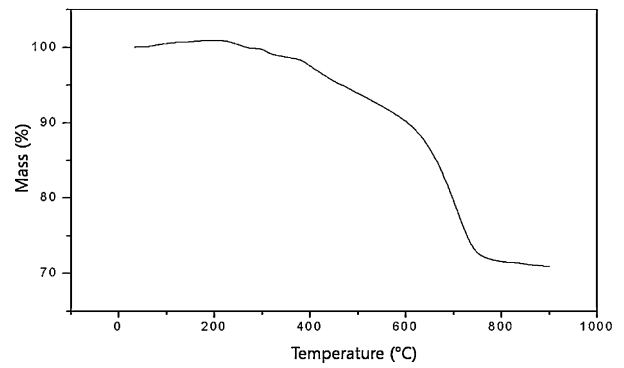
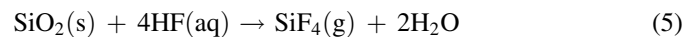


Fig. 4. TG curve of synthesized SiC powder from N-1.

ture is increased from 100 to 900 °C at a heating rate of 10 °C/min in an air atmosphere. The weight loss that occurred from 200 °C to 750 °C resulted from the oxidation of the free carbon. The free carbon was driven off to obtain pure SiC nano-powder by a heat treatment at 800 °C. The free carbon treatment reaction can be described as follows:



Fig. 5 shows the XRD pattern of the powders produced by the heat treatment. The major peaks of the  $\beta$ -SiC phase and some minor amount of the  $\alpha$ -SiC phase can be observed. At the same time, the amorphous  $\text{SiO}_2$  phase is detected at a diffraction angle of nearly 22°. Amorphous  $\text{SiO}_2$  was produced due to the oxidation of silicon carbide on the surfaces of the particles during the heat treatment at 800 °C [17]. Amorphous  $\text{SiO}_2$  was driven off by a HF treatment. The HF treatment reaction can be described as follows:



A XRD pattern of powders produced by HF treatment is shown in Fig. 6. The XRD patterns of all synthesized powders clearly showed the existence of the  $\beta$ -SiC and  $\alpha$ -SiC phases, and no

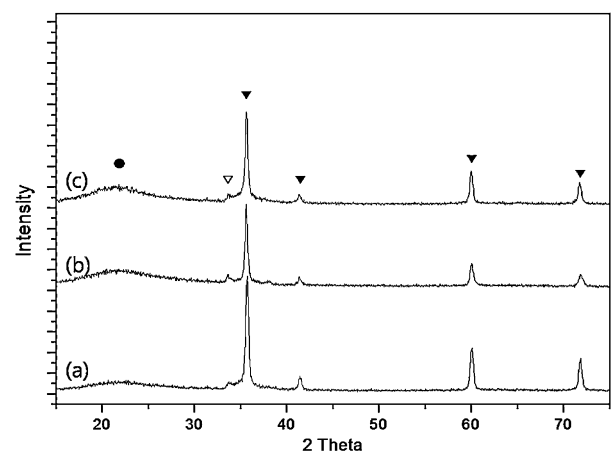


Fig. 5. X-ray diffraction patterns of synthesized SiC nano-powders after heat treatment: (a) N-1, (b) N-2, and (c) N-3.

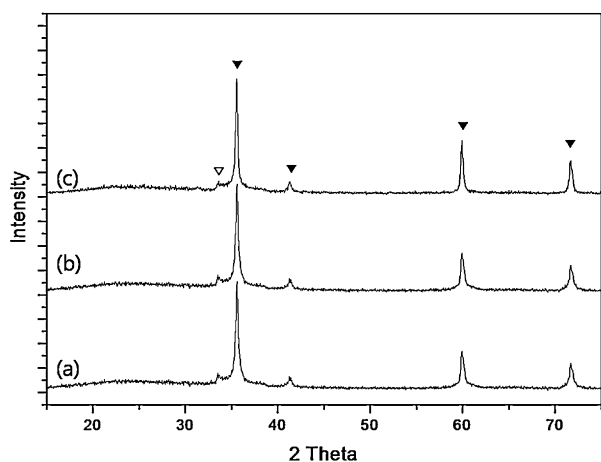


Fig. 6. X-ray diffraction patterns of synthesized SiC nano-powders after HF treatment: (a) N-1, (b) N-2, and (c) N-3.

indication of an impurity phase was observed. Pure SiC nano-powder was obtained after the heat and HF treatment.

#### 4. Conclusions

In this paper, nano-silicon carbide powders are synthesized from organic precursors by RF inductively coupled thermal plasma. Commercially available tetraethylorthosilicate, hexamethyldisilazane and vinyltrimethoxysilane were used as the precursor materials.

The XRD patterns of all of the synthesized powders showed the  $\beta$ -SiC,  $\alpha$ -SiC and the free carbon phases. The synthesized powders had particle sizes in the range of 30–100 nm. The morphology of the synthesized powders was with globular and hexagonal.

The synthesized powders consisted of SiC with free carbon and amorphous silica ( $\text{SiO}_2$ ). After a thermal treatment and a HF treatment, the impurities were driven off resulting in pure SiC nano-powder.

#### Acknowledgement

This research was supported by a grant from the Fundamental R;D Program for Technology of World Premier Materials funded by the Ministry of Knowledge Economy, Republic of Korea.

#### References

- [1] M. Pierre, Silicon carbide and silicon carbide-based structures: the physics of epitaxy, *Surf. Sci. Rep.* 48 (1–4) (2002) 1–51.
- [2] Q.G. Fu, H.J. Li, X.H. Shi, K.Z. Li, G.D. Sun, Silicon carbide coating to protect carbon/carbon composites against oxidation, *Scr. Mater.* 52 (2005) 923–927.
- [3] B.G. Ravi, O.A. Omotoye, T.S. Srivatsan, M. Petrorali, T.S. Sudarshan, The microstructure and hardness of silicon carbide synthesized by plasma pressure compaction, *J. Alloys Compd.* 299 (2009) 292–296.
- [4] A. Chrysanthou, P. Grieveson, Formation of silicon carbide whiskers and their microstructure, *J. Mater. Sci.* 26 (1991) 3463–3476.
- [5] Y. Zhong, L. Shaw, M. Manjarres, M.F. Zawrah, Synthesis of silicon carbide nanopowder using silica fume, *J. Am. Ceram. Soc.* 93 (2010) 3159–3167.
- [6] I.N. Kholmanov, A. Kharlamov, E. Barborini, C. Lenardi, A.L. Bassi, C.E. Bottani, C. Ducati, S. Maffi, N.V. Kirillova, P. Milani, A simple method for the synthesis of silicon carbide nanorods, *J. Nanosci. Nanotechnol.* 2 (2002) 453–456.
- [7] D.K. Kim, S. Park, K. Cho, H.B. Lee, Synthesis of SiC by self-propagating high temperature synthesis chemical furnace, *J. Korean Ceram. Soc.* 31 (1994) 1283–1292.
- [8] L.N. Satapathy, P.D. Ramesh, D. Agrawal, R. Roy, Microwave synthesis of phase-pure, fine silicon carbide powder, *Mater. Res. Bull.* 40 (2005) 1871–1882.
- [9] N. Kobayashi, Y. Kawakami, K. Kamada, J.G. Li, R. Ye, T. Watanabe, T. Ishigaki, Spherical submicron-size copper powders coagulated from a vapor phase in RF induction thermal plasma, *Thin Solid Films* 516 (2008) 4402–4406.
- [10] M. Leparoux, Y. Kihn, S. Paris, C. Schreuders, Microstructure analysis of RF plasma synthesized TiCN nanopowders, *Int. J. Refract. Met. Hard Mater.* 26 (2008) 277–285.
- [11] T. Ishigaki, S.M. Oh, J.G. Li, D.W. Park, Controlling the synthesis of TaC nanopowders by injecting liquid precursor into RF induction plasma, *Sci. Technol. Adv. Mater.* 6 (2005) 111–118.
- [12] R. Ye, J.G. Li, T. Ishigaki, Controlled synthesis of alumina nanoparticles using inductively coupled thermal plasma with enhanced quenching, *Thin Solid Films* 515 (2007) 4251–4257.
- [13] Z. Karoly, J. Szepvolgyi, Z. Farkas, Simultaneous calcinations and spheroidization of gibbsite powders in an RF thermal plasma, *Powder Technol.* 110 (2000) 169–178.
- [14] L.R. Tong, R.G. Reddy, Synthesis of titanium carbide nano-powders by thermal plasma, *Scr. Mater.* 52 (2005) 1253–1258.
- [15] H.P. Klug, L.E. Alexander, X-ray Diffraction Procedures for Polycrystalline and Amorphous Materials, Wiley, New York, 1974.
- [16] J. Szepvolgyi, I. Mohai, Z. Karoly, L. Gal, Synthesis of nano sized ceramic powders in a radio frequency thermal plasma reactor, *J. Eur. Ceram. Soc.* 28 (2008) 895–899.
- [17] L. Shi, H. Zhao, Y. Yan, Z. Li, C. Tang, Synthesis and characterization of submicron silicon carbide powders with silicon and phenolic resin, *Powder Technol.* 169 (2006) 71–76.